

1 Supplement S1

2 Calculation of phototrophic energy fluxes per unit mass at different light levels

3 The ‘return on investment’ of a phototrophic system is taken in this work to be the energy flux
4 per unit mass of the dedicated phototrophic machinery at a given light level. Recycling rate of
5 individual proteins within the phototrophic machinery was beyond the scope of this review to
6 incorporate due to the widely varying half-life or dilution rates of different components, and as
7 such energy fluxes are measured in energy flux per unit mass rather than energy yield per unit of
8 protein synthesis.

9 To calculate the maximum mass-specific energetic rate of return (V_{max}) on investment of
10 retinalophototrophic versus chlorophototrophic systems, the total mass per functional
11 phototrophic unit (M_{total}), the cycling rate (R_{max}), and the protons pumped per cycle (N_p) must be
12 known. V_{max} is equal to the product of N_p and R_{max} divided by M_{total} , as described in the
13 following equation:

Equation 1: $V_{max} = N_p \cdot R_{max} / M_{total}$

15 Two retinalophototrophic systems, bacteriorhodopsin and proteorhodopsin, and two
16 chlorophototrophic systems, oxygenic photosynthesizers and purple bacteria, were considered
17 for breadth. Bacteriorhodopsin is described as a functionally monomeric 26 kDa protein [1] and
18 proteorhodopsin is described as a functionally monomeric 27 kDa protein [2].

19 In the case of complex chlorophototrophic systems, the total mass per functional phototrophic
20 unit must be calculated to include the mass of any antenna complexes associated with a

21 chlorophototrophic reaction center. This was done by multiplying the mass of each antenna
22 complex by the number of antenna complexes per photosynthetic unit at their in vivo
23 stoichiometry, and adding this to the total mass of the active center. There are few cases in
24 which every reaction center and antenna complex in a single organism are structurally
25 understood and the stoichiometry of each component is known. Thus, in order to estimate the
26 total mass of a functional unit of chlorophototrophic machinery it is necessary to use data from
27 multiple functionally similar organisms to infer an approximate value.

28 An oxygenic chlorophototrophic reaction center was taken to be a single instance of either
29 photosystem I (PSI) or photosystem II (PSII). As described in Cunningham et al., 1989 [3], the
30 ratio of PSII : PSI : Phycobilisome in the oxygenic red algae *Porphyridium cruentum* (ATCC
31 50161) in low light ($6 \mu\text{mol photons m}^{-2} \text{ s}^{-1}$) is $2.85 : 5.35 : 1$ and in high light ($280 \mu\text{mol}$
32 $\text{photons m}^{-2} \text{ s}^{-1}$) the ratio is $3.96 : 7.59 : 1$. The average across all conditions tested was 3.13
33 PSII : 6.50 PSI : 1 phycobilisome in this red algae. The mass of PSII is taken to be 350 kDa as
34 described for *Thermosynechococcus vulcanis* in Umena et al., 2011 [4], the mass of PSI is taken
35 to be 356 kDa as described for *Synechococcus elongatus* in Fromme et al., 2001 [5], and the
36 mass of a phycobilisome antenna complex is taken to be 16.2 mDa as described for the red algae
37 *Griffithsia pacifica* in Zhang et al., 2017 [6]. This brings the total mass of an approximated
38 stoichiometric unit with 9.63 reaction centers (RCs) and one phycobilisome to approximately
39 20.2 mDa and the total mass per reaction center to 2098 kDa .

40 The mass of antenna complexes other than phycobilisomes in oxygenic chlorophototrophs was
41 not considered due to diversity in antenna complexes present in different organisms. The mass
42 of other electron transport chain components or membrane ATPases was not considered due to

43 likely low but poorly constrained stoichiometries [7], low masses compared to phycobilisomes
44 [8], and their use in multiple cellular processes compared to the comparatively dedicated
45 chlorophototrophic machinery.

46 Table S1: Mass estimation per oxygenic chlorophototrophic reaction center

Component	Number per stoichiometric unit	Mass
PSII	3.13	350 kDa
PSI	6.50	356 kDa
Phycobilisome	1	16.2 mDa
Total (9.63 RC plus phycobilisome)		20.2 mDa
Mass per RC (M_{total})		2098 kDa

47 A representative anoxygenic chlorophototrophic system from the purple bacteria species
48 *Rhodospirillum photometricum* was examined for comparison, as described by Scheuring &
49 Sturgis, 2009 [9]. In this species, each type-II reaction center is associated with one complex of
50 16 LH1 antenna proteins, forming a ‘core complex’, and multiple rings of 9 LH2 antenna
51 proteins. The core complex:LH2 complex ratio was taken to be 3.5, as observed at high light
52 adaptation in this work. The mass of the RCII/LH1 core complex described in Niwa et al., 2014
53 [10] in the purple bacterium *Thermochromatium tepidum* is 380 kDa. The measured mass of the
54 LH2 complex described by Cherezov et al., 2006 [11] in the purple bacterium *Rps acidophila* is
55 130 kDa. This brings the total mass of a stoichiometric unit containing a single RC to
56 approximately 835 kDa. Again, the mass of additional electron transport chain components was

57 not considered due to the multiple roles of these components in other cellular processes and low
58 apparent stoichiometry relative to other chlorophototrophic machinery [7].

59 Table S2: Mass estimation per anoxygenic purple bacteria chlorophototrophic reaction center

Component	Number per stoichiometric unit	Mass
RC + LH1	1	380 kDa
LH2	3.5	130 kDa
Mass per RC (M_{total})		835 kDa

60 Field measurements of the maximum cycling rate of chlorophototrophic reaction centers from
61 Kolber et al., 2000 [12] were used along with these figures to estimate the maximum energy flux
62 per unit protein available to chlorophototrophs. In saturating light levels, oxygenic phototrophic
63 phytoplankton were measured to have a maximum sustainable rate of reaction center
64 photocycling of approximately 350 per second, and aerobic anoxygenic phototrophs were
65 measured to reach up to approximately 150 per second. These are broadly consistent with in
66 vitro measurements of photosystem II photocycle rate of more than 200 cycles per second
67 observed in isolated photosystems by Lubner et al., 2011 [13]. Each photocycle of a reaction
68 center was taken to represent two protons pumped across the photosynthetic membrane by the
69 cytochrome b₆f complex in oxygenic chlorophototrophs or other electron transport chain
70 components in anoxygenic chlorophototrophs. Electron transport chains containing the
71 Complex-I like NDH complex (likely capable of pumping additional protons) rather than
72 cytochrome b₆f alone was not considered due to a low apparent rate of cycling and low

73 stoichiometry, suggesting that while necessary for regulatory purposes it is not a primary player
74 in energy metabolism [14].

75 Microbial rhodopsins were represented by proteorhodopsin which has been measured at being
76 capable of 25 pumping protons per second in Friedrich et al., 2002 [15] and bacteriorhodopsin
77 measured at approximately 50-100 protons per second in Béja et al., 2000 [2] and Lanyi, 2006
78 [16]. We conservatively took the bacteriorhodopsin maximum cycling rate to be 50 protons per
79 second. In all cases, energy flux was calculated as described in equation 1.

80 Table S3: Maximum energy flux per unit mass for chlorophototrophy and retinalophototrophy

	Proteorhodopsin	Bacteriorhodopsin	Oxygenic RC	Anoxygenic RC
M _{total} (kDa)	27	26	2098	835
R _{max} (cycles s ⁻¹)	25	50	350	150
N _p (protons cycle ⁻¹)	1	1	2	2
R _{max} *N _p (Protons s ⁻¹)	25	50	700	300
V _{max} (Protons kDa ⁻¹ s ⁻¹)	0.93	1.92	0.33	0.36

81 The response of the energy flux per kilodalton of protein mass in chlorophototrophs and
82 retinalophototrophs to varying light levels was modeled via simple Michaelis–Menten kinetics,
83 using the following equation:

84 Equation 2: $V = \frac{V_{max} \cdot [lightintensity]}{K_m + [lightintensity]}$

85 V_{max} was taken to be the previously calculated maximum energy flux rate of a phototrophic
86 system in protons $kDa^{-1} s^{-1}$. K_m represents the light level at which the energy flux per functional
87 unit reaches its half-maximum. The K_m for both proteorhodopsin and bacteriorhodopsin was
88 taken to be $2700 \mu mol m^{-2} s^{-1}$, as described for proteorhodopsin in Walter et al., 2007 [17]. The
89 K_m for oxygenic RCs was taken to be $40 \mu mol m^{-2} s^{-1}$ and the K_m for an anoxygenic RC was
90 taken to be $191 \mu mol m^{-2} s^{-1}$, as described in Kirchman and Hanson, 2013 [18].

91 Table S4: K_m , V_{max} for energy flux per unit mass for chlorophototrophy and retinalophototrophy

	Proteorhodopsin	Bacteriorhodopsin	Oxygenic RC	Anoxygenic RC
$K_m (\mu mol m^{-2} s^{-1})$	2700	2700	40	191
V_{max} (Protons $kDa^{-1} s^{-1}$)	0.93	1.92	0.33	0.36

92 The relationship between light intensity and the energy flux per unit incident light for each
93 phototrophic system was calculated using equation 3, derived by dividing Equation 2 by [light
94 intensity], yielding the following equation.

95 Equation 3:
$$Y = \frac{V_{max}}{K_m + [lightintensity]}$$

96 The yield Y , in units of protons $kDa^{-1} s^{-1}$ / ($\mu mol m^{-2} s^{-1}$), represents the specific energy flux of a
97 unit of protein machinery per unit incident light, and is reduced upon saturation of the machinery
98 with light. It is thus maximized at low light. The form that this efficiency curve takes is similar
99 to that determined from first-principles modeling of anoxygenic chlorophototrophic machinery in
100 Sener et al., 2019 [19].

101 The maximum yield per unit incident light was calculated by setting [light intensity] equal to
102 zero, at which point the value of Equation 3 is maximized and the largest marginal return per unit
103 incident light is achieved. This value is represented by the following equation:

104
$$\text{Equation 4: } Y_{max} = V_{max}/K_m$$

105 This maximum yield represents the highest efficiency available per available light resource,
106 reached at infinitesimal light levels.

107 Table S5: Maximum yield Y_{max} for chlorophototrophy and retinalophototrophy

	Proteorhodopsin	Bacteriorhodopsin	Oxygenic RC	Anoxygenic RC
Y_{max} (protons $\text{kDa}^{-1} \text{s}^{-1}$ / $(\mu\text{mol m}^{-2} \text{s}^{-1})$)	3.43×10^{-4}	7.12×10^{-4}	8.34×10^{-3}	1.88×10^{-3}

108 It is important to note that a large fraction of the difference in efficiency per unit incident light
109 between chlorophototrophic and retinalophototrophic machinery is due not to the greater
110 quantum yield of chlorophototrophic machinery per unit absorbed photon, but instead is simply
111 due to a much larger absorption cross section per functional unit due to a much larger amount of
112 dedicated light-gathering protein machinery per unit. However, the total absorption cross section
113 per unit infrastructure for chlorophototrophs and retinalophototrophs is quite similar.

114 The protein infrastructure mass per unit absorption (M_{cs}) of a phototrophic system measures how
115 efficiently light is captured. It is calculated from the mass per functional unit (M_{total}) and the
116 absorption cross section per functional unit (C_s). The cross-section per functional unit is taken

117 from Kirchman and Hanson, 2013 [18], in which it is approximated for all rhodopsins (2 \AA^2), an
118 oxygenic phototroph (100 \AA^2), and an anoxygenic phototroph (50 \AA^2) based on a compilation of
119 experiments and the light spectrum available in a marine environment. This is represented by the
120 following equation:

121
$$\text{Equation 5: } M_{cs} = M_{total}/Cs$$

122 The mass per unit light-absorbing cross section is measured in in units of kDa \AA^{-2} .

123 While a large amount of the difference in efficiency per unit incident light is explicable in terms
124 of the difference in total mass per functional unit, the enhanced quantum yield of
125 chlorophototrophic machinery in terms of protons pumped per photon absorbed is an important
126 difference between the two forms of phototrophy. Thus, to account for the greater yield per
127 absorbed photon, the mass per unit cross section is normalized using the following equation:

128
$$\text{Equation 6: } \text{Normalized } M_{cs} = M_{cs}/\text{Yield}$$

129 This normalized mass per unit cross section accounts for the fact that photons absorbed by
130 chlorophototrophic machinery are used to energize an electron transport chain and are capable of
131 pumping ~ 2 protons per photon rather than the 1 proton per photon of retinalophototrophic
132 machinery, and are thus twice as efficient in terms of yield per unit incident light.

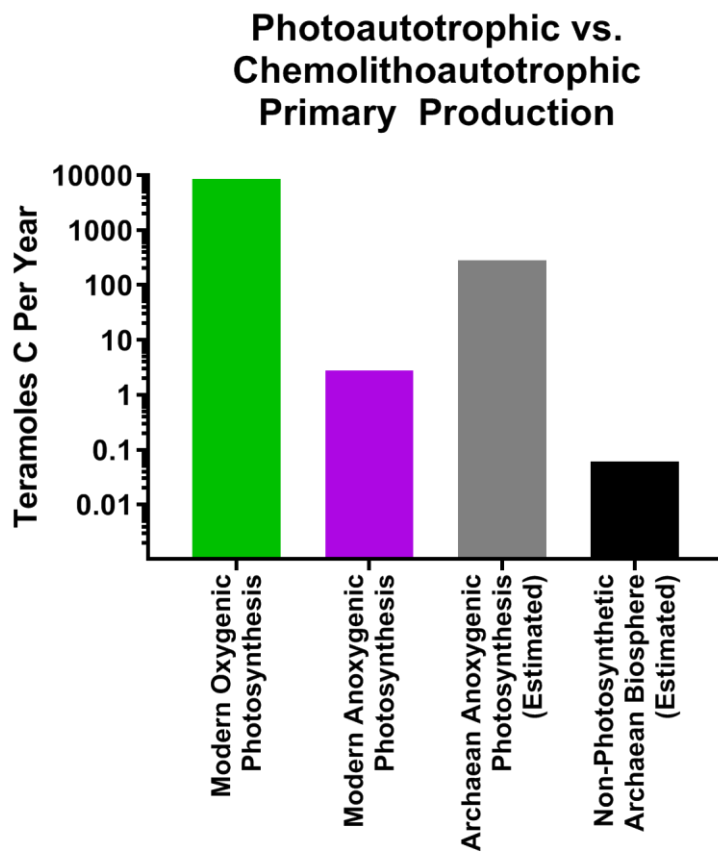
133 Table S6: mass per unit cross section calculation for chlorophototrophy and retinalophototrophy

	Proteorhodopsin	Bacteriorhodopsin	Oxygenic RC	Anoxygenic RC
M_{total} (kDa)	27	26	2098	835

$C_s (\text{\AA}^2)$	2	2	100	50
$M_{cs} (\text{kDa \AA}^{-2})$	13.5	13	20.98	16.7
Yield (protons/photon)	1	1	2	2
Yield-Normalized $M_{cs} (\text{kDa \AA}^{-2})$	13.5	13	10.49	8.35

134 Strikingly, the mass per unit cross section for all phototrophic machineries, chlorophototrophic
 135 and retinalophototrophic, are calculated to be within a factor of ~1.6 regardless of yield
 136 normalization. This suggests that this approximate level of absorption cross section per unit
 137 mass represents a biophysical constraint of proteins bound to optically active cofactors, rather
 138 than being a detail specific to each form of phototrophic machinery (see Supplemental Figure 2).
 139 This may, however, be violated in the case of anoxygenic phototrophs bearing chlorosomes – the
 140 protein mass per chlorophyll molecule in these specialized structures present in bacteria adapted
 141 for extremely low-light conditions is estimated to be less than one fifth that of other
 142 chlorophototrophs [20]. These extreme low-light adapted phototrophs likely extend the trade-off
 143 between efficiency per unit resource and efficiency per unit light beyond that observed in other
 144 chlorophototrophs, as the mass per functional unit rises drastically while capturing dimmer light.
 145

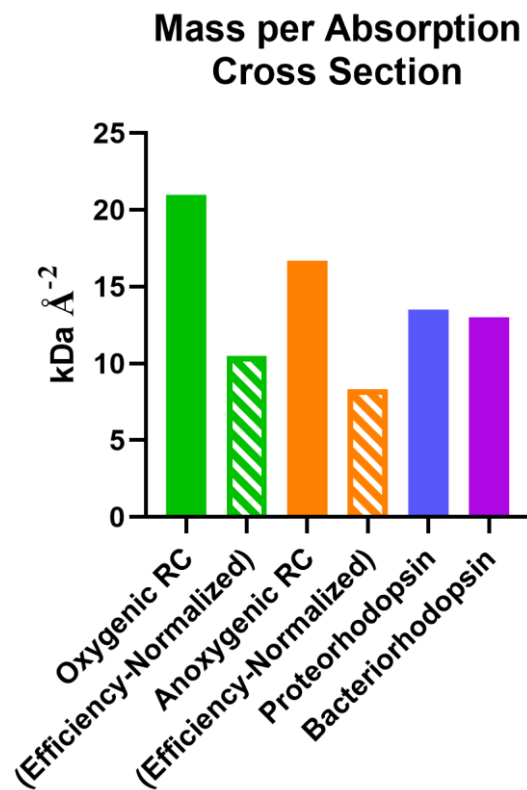
146 Supplemental Figure 1:



147

148 Legend: Comparison between carbon flux through biospheres driven by photosynthesis and
149 chemolithoautotrophy. Modern oxygenic photosynthesis drives carbon fixation of nearly 9,000
150 teramoles per year [21]. While modern anoxygenic photosynthesis represents at most ~2.7
151 teramoles per year [22], estimates of anoxygenic photosynthesis in the Archaean are ~280
152 teramoles per year [23]. Estimates of possible carbon flux through a pre-photosynthetic, entirely
153 chemolithotrophic biosphere driven by Archaean geochemical fluxes alone are circa 0.06
154 teramoles per year [24].

155 Supplemental Figure 2:



156

157 Legend: In solid colors, the mass per unit absorption cross section of chlorophototrophic and
158 retinalphototrophic machinery as calculated from table S6. In striped colors, the yield-
159 normalized mass per unit absorption cross section. Chlorophototrophic machinery is slightly
160 more massive per unit light absorbed before normalization for quantum yield, and slightly less
161 massive per unit light absorbed after normalization. No systems vary by more than
162 approximately a factor of 1.6.

163

164 Works Cited:

165 1. Oesterhelt, D. and W. Stoeckenius, *Rhodopsin-like protein from the purple membrane of*
166 *Halobacterium halobium*. *Nature new biology*, 1971. **233**(39): p. 149-152.

167 2. Béja, O., et al., *Bacterial rhodopsin: evidence for a new type of phototrophy in the sea*. *Science*,
168 2000. **289**(5486): p. 1902-1906.

169 3. Cunningham, F.X., et al., *Stoichiometry of photosystem I, photosystem II, and phycobilisomes in*
170 *the red alga Porphyridium cruentum as a function of growth irradiance*. *Plant physiology*, 1989.
171 **91**(3): p. 1179-1187.

172 4. Umena, Y., et al., *Crystal structure of oxygen-evolving photosystem II at a resolution of 1.9 Å*.
173 *Nature*, 2011. **473**(7345): p. 55-60.

174 5. Fromme, P., P. Jordan, and N. Krauß, *Structure of photosystem I*. *Biochimica et Biophysica Acta*
175 (BBA)-Bioenergetics, 2001. **1507**(1-3): p. 5-31.

176 6. Zhang, J., et al., *Structure of phycobilisome from the red alga Griffithsia pacifica*. *Nature*, 2017.
177 **551**(7678): p. 57-63.

178 7. Singharoy, A., et al., *Atoms to Phenotypes: Molecular Design Principles of Cellular Energy*
179 *Metabolism*. *Cell*, 2019. **179**(5): p. 1098-1111. e23.

180 8. Muench, S.P., J. Trinick, and M.A. Harrison, *Structural divergence of the rotary ATPases*.
181 *Quarterly reviews of biophysics*, 2011. **44**(3): p. 311-356.

182 9. Scheuring, S. and J.N. Sturgis, *Atomic force microscopy of the bacterial photosynthetic*
183 *apparatus: plain pictures of an elaborate machinery*. *Photosynthesis research*, 2009. **102**(2-3): p.
184 197-211.

185 10. Niwa, S., et al., *Structure of the LH1-RC complex from Thermochromatium tepidum at 3.0 Å*.
186 *Nature*, 2014. **508**(7495): p. 228-232.

187 11. Cherezov, V., et al., *Room to move: crystallizing membrane proteins in swollen lipidic*
188 *mesophases*. *Journal of molecular biology*, 2006. **357**(5): p. 1605-1618.

189 12. Kolber, Z.S., et al., *Bacterial photosynthesis in surface waters of the open ocean*. *Nature*, 2000.
190 **407**(6801): p. 177-179.

191 13. Lubner, C.E., et al., *Solar hydrogen-producing bionanodevice outperforms natural*
192 *photosynthesis*. *Proceedings of the National Academy of Sciences*, 2011. **108**(52): p. 20988-
193 20991.

194 14. Nawrocki, W., et al., *The mechanism of cyclic electron flow*. *Biochimica et Biophysica Acta (BBA)-*
195 *Bioenergetics*, 2019.

196 15. Friedrich, T., et al., *Proteorhodopsin is a light-driven proton pump with variable vectoriality*.
197 *Journal of molecular biology*, 2002. **321**(5): p. 821-838.

198 16. Lanyi, J.K., *Proton transfers in the bacteriorhodopsin photocycle*. *Biochimica et Biophysica Acta*
199 *(BBA)-Bioenergetics*, 2006. **1757**(8): p. 1012-1018.

200 17. Walter, J.M., et al., *Light-powering Escherichia coli with proteorhodopsin*. *Proceedings of the*
201 *National Academy of Sciences*, 2007. **104**(7): p. 2408-2412.

202 18. Kirchman, D.L. and T.E. Hanson, *Bioenergetics of photoheterotrophic bacteria in the oceans*.
203 *Environmental microbiology reports*, 2013. **5**(2): p. 188-199.

204 19. Sener, M., et al., *Overall energy conversion efficiency of a photosynthetic vesicle*. *elife*, 2016. **5**:
205 p. e09541.

206 20. Bryant, D.A. and D.P. Canniffe, *How nature designs light-harvesting antenna systems: design*
207 *principles and functional realization in chlorophototrophic prokaryotes*. *Journal of Physics B:*
208 *Atomic, Molecular and Optical Physics*, 2018. **51**(3): p. 033001.

209 21. Field, C.B., et al., *Primary production of the biosphere: integrating terrestrial and oceanic*
210 *components*. *science*, 1998. **281**(5374): p. 237-240.

211 22. Raven, J.A., *Contributions of anoxygenic and oxygenic phototrophy and chemolithotrophy to*
212 *carbon and oxygen fluxes in aquatic environments*. Aquatic Microbial Ecology, 2009. **56**(2-3): p.
213 177-192.

214 23. Canfield, D.E., M.T. Rosing, and C. Bjerrum, *Early anaerobic metabolisms*. Philosophical
215 Transactions of the Royal Society B: Biological Sciences, 2006. **361**(1474): p. 1819-1836.

216 24. Sleep, N.H. and D.K. Bird, *Niches of the pre-photosynthetic biosphere and geologic preservation*
217 *of Earth's earliest ecology*. Geobiology, 2007. **5**(2): p. 101-117.

218